

Temperature dependence of dark current in a CCD

Ralf Widenhorn,[†] Morley M. Blouke,^{*} Alexander Weber, Armin Rest,^{**} Erik Bodegom[‡]

Department of Physics, Portland State University, Portland, OR 97207

^{*}Scientific Imaging Technologies, Tigard, OR 97223,

^{**}Astronomy Department, University of Washington, Seattle, WA 98195

ABSTRACT

We present data for dark current of a back-illuminated CCD over the temperature range of 222 to 291 K. Using an Arrhenius law, we found that the analysis of the data leads to the relation between the prefactor and the apparent activation energy as described by the Meyer-Neldel rule. However, a more detailed analysis shows that the activation energy for the dark current changes in the temperature range investigated. This transition can be explained by the larger relative importance at high temperatures of the diffusion dark current and at low temperatures by the depletion dark current. The diffusion dark current, characterized by the band gap of silicon, is uniform for all pixels. At low temperatures, the depletion dark current, characterized by half the band gap, prevails, but it varies for different pixels. Dark current spikes are pronounced at low temperatures and can be explained by large concentrations of deep level impurities in those particular pixels. We show that fitting the data with the impurity concentration as the only variable can explain the dark current characteristics of all the pixels on the chip.

Keywords: depletion dark current, diffusion dark current, Meyer-Neldel rule

1. INTRODUCTION

Since the invention of the Charged-Coupled Device (CCD) in 1969, by George E. Smith and Willard S. Boyle at the Bell Telephone Laboratories, the CCD technology has come a long way. State of the art CCDs are able to detect light levels of a few photons. The detection of photons is done by capturing the photoelectrons, generated by the photoelectric effect, in a potential well. For low light level applications only a few signal electrons are generated and the noise limits the resolution of the CCD. A source of noise intrinsic to the CCD is the so-called dark current. It is generated even though the chip is not exposed to light. This dark current is due to the thermal excitation of electrons into the conduction band and collection in the CCD wells. The generation of dark electrons is a thermally activated process and as such strongly temperature dependent. One way to suppress dark current is by cooling the CCD-chip to very low temperatures. Dark current is not uniform for all pixels. Pixels with a very high dark signal are referred to as dark current spikes or hot pixels. They are generally randomly distributed and show up as white dots in a dark frame (Fig. 1). Pictures containing dark current can be corrected by subtracting a dark frame of the same exposure time from the image. However, subtracting a dark frame adds the Poison noise of this frame to the image.

We investigated the dark current for a backside-illuminated CCD housed in SpectraVideo camera (Model: SV512V1) manufactured by Pixelvision, Inc.. The chip was a three phase, n-buried channel, three-level polysilicon back-thinned device (12.3 mm x 12.3 mm, 512 x 512 pixels, manufactured by SITE Inc.) with an individual pixel size of 24 μm x 24 μm . The outer edge (20 pixels) was excluded from the analysis. In order to minimize uncertainties due to the readout noise and the Poison noise, the dark current was determined as the average of several pictures. 50 images were taken each for the following exposure times: 3, 5, 10, 20, 50, 100 s, 20 images each for 250 and 500 s and 10 images were taken for 1000 s. Dark frames for all exposure times were taken at 222, 232, 242, 252 and 262 K, for exposure times up to 500 s at 271 K, for exposure times up to 250 s at 281 K and for exposure times up to 50 s at 291 K. None of the of 472 x 472 pixel subframes showed pixels which were saturated and the dark current increased linearly with increasing exposure time. Hence, we could calculate the dark current by fitting the number of electrons collected versus the exposure time.¹

[†] Electronic mail: ralfw@pdx.edu

[‡] Electronic mail: bodegom@pdx.edu

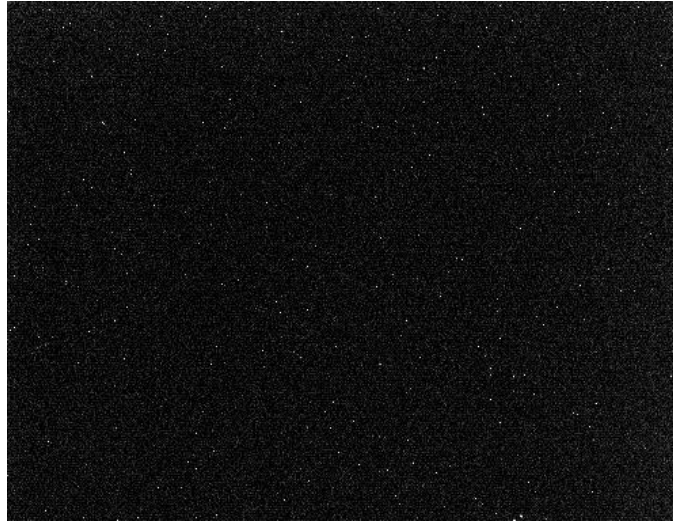


FIG. 1. 20 seconds dark frame taken at 252 K. The white dots represent pixels with high dark current. They are often referred to as hot pixels or dark current spikes.

2. THE MEYER-NELDEL RULE FOR DARK CURRENT IN A CCD

In a first approach the dark current, as many thermally activated processes, was assumed to follow the Arrhenius law:

$$De^- = De_0^- \exp(-\Delta E/kT), \quad (1)$$

where De^- is the dark current in e^-/s and ΔE is the activation energy. According to Eq. (1) all data points in a plot of the logarithm of De^- versus the inverse temperature, the so-called Arrhenius plot, should lay on a straight line. The activation energy of the process is the absolute value of the slope of this line. Figure 2 shows the Arrhenius plot and linear fits to the data points of four random pixels. Although a straight line fit does not model the data perfectly, the assumption of describing dark current with Eq. (1) seems reasonable. We fitted all 222,784 individual pixels according to the Arrhenius law and obtained 222,784 pairs of exponential prefactors, De_0^- , and activation energies ΔE . These results were analyzed according to the Meyer-Neldel rule (MNR).

The MNR is an empirical law first espoused by W. Meyer and H. Neldel in 1937, and is observed frequently for processes which follow the Arrhenius law.² The rule states that the logarithm of the exponential prefactor depends linearly on the activation energy. Hence, for the dark current:

$$De_0^- = De_{00}^- \exp(\Delta E/E_{MN}), \quad (2)$$

where De_{00}^- and E_{MN} are positive constants. The MNR is found in various fields and for several different processes, e.g. for diffusion^{3,4} or the conductivity of semiconductors.⁵⁻⁷ Although different explanations have been proposed none is universally accepted and the discussion as to what causes the MNR is not settled. It has been argued that the MNR arises due to an exponential density of state distribution that induces a shift in the Fermi level.⁸ Others see the origin in the entropy of multiple excitations.^{9,10}

The CCD gives the unique possibility to investigate the MNR for a set of more than 222,000 samples. Figure 3 shows the plot of the logarithm of the exponential prefactor versus the activation energy for all pixels. The activation energies vary from roughly half the band-gap of Si to about the band-gap of Si, with most pixels having ΔE 's of approximately 0.9 eV to 1 eV. The agreement of all data points with the MNR is remarkable. We can deduce the two MNR-constants

as $E_{MN}=25.3$ meV and $De_{00}^- = 1685$ e/s. In order to get a better understanding of the meaning of these two constants substituting Eq. (2) into Eq. (1) one obtains:

$$De^- = De_{00}^- \exp\left[\Delta E\left(\frac{1}{E_{MN}} - \frac{1}{kT}\right)\right] \quad (3)$$

Eq. (3) shows that for a characteristic temperature or energy the dark current is independent of the activation energy. This temperature, also known as isokinetic temperature, is given for our experiment as $T_{MN}=E_{MN}/k=294$ K. De_{00}^- is the dark current at this particular temperature. The isokinetic temperature can also be seen in Fig. 2 as the intersection of the linear fits. The agreement of the linear fits and the actual data points at T_{MN} is not perfect. At temperatures higher than the isokinetic temperature the MNR predicts an inversion of the dark current. Hence, hot pixels with a high dark current at low temperature should show a lower dark current than other pixels for $T>T_{MN}$. In order to verify this prediction, the chip was heated to a temperature of 313 K. We found that the predicted inversion did not occur. It could only be found that the dark current was fairly similar for all pixels. As we will show later this is not surprising, but to be expected for dark current in a CCD.

Thus, the linear relationship between the logarithm of the prefactor and the activation energy for all 222,784 pixels is remarkable, but the MNR does not predict the dark current close to and above the isokinetic temperature accurately. In fact the apparent crossing in the Arrhenius plot is actually more a convergence of the dark currents for different pixels. A closer look at the data-set shows a positive curvature in the Arrhenius plot. The activation energy is lower at low temperatures than at high temperatures. We showed that such a change in the activation energy can explain the observation of the MNR.¹¹ The origin of the shift in the activation energy with changing temperature for dark current in a CCD will be discussed in the next section.

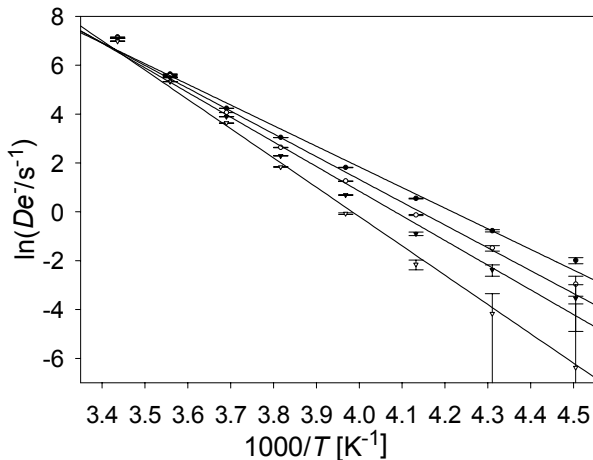


FIG. 2 The logarithm of the dark current vs the inverse temperature and linear fits for four different pixels.

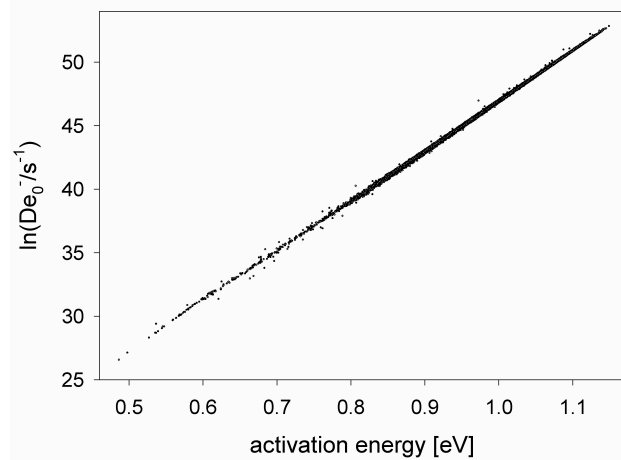


FIG. 3 The logarithm of the exponential prefactor vs the apparent activation energy for all pixels on the CCD-chip.

3. SOURCES OF DARK CURRENT

The dark current in a CCD is a very important source of noise and has been studied thoroughly. Generally three different sources of dark current contribute to the total dark current in a CCD: the depletion or bulk dark current generated in the depletion region, the diffusion dark current generated in the field-free region and the surface dark current generated at the Si-SiO₂ interface. For a CCD operated in multipinned phase (MPP) mode the interface is

inverted with a high hole carrier concentration and this source of dark current is almost completely suppressed. The analysis of the remaining diffusion and depletion dark current is very similar to the analysis of the dark current in a diode and can be found in various books on semiconductors, see for example Grove¹² or Sze.¹⁶ The generation or recombination of an electron-hole pair can occur either as a band-to-band process (i.e., conduction band to valence band) or through an intermediate state. The band-to-band process should only depend on the band structure of the semiconductor. However, it has been found that the generation or recombination of carriers in Si depends greatly on the preparation of the semiconductor. This indicates that the recombination and generation process involves impurities or imperfections. Those imperfections disrupt the lattice of Si and introduce energy levels into the band-gap. The net generation-recombination rate, U , of carriers through these intermediate centers has been successfully described by Hall, Shockley and by Read.¹³⁻¹⁵ It can be shown that:

$$U = \frac{\sigma_p \sigma_n v_{th} (pn - n_i^2) N_t}{\sigma_n \left[n + n_i \exp\left(\frac{E_t - E_i}{kT}\right) \right] + \sigma_p \left[p + n_i \exp\left(\frac{E_i - E_t}{kT}\right) \right]}, \quad (4)$$

where σ_p and σ_n are the capture cross-sections for holes and electrons respectively, v_{th} the thermal velocity, n the electron concentration, p the hole concentration, N_t the concentration of bulk generation-recombination centers at the energy level E_t , E_i the intrinsic Fermi level and n_i the intrinsic carrier concentration which is given as:

$$n_i = \sqrt{N_v N_c} \exp(-E_g/2kT), \quad (5)$$

where E_g stands for the band gap in silicon and N_v and N_c are the effective density of states for the valence and conduction band respectively. In thermal equilibrium, $pn = n_i^2$ and thus the generation is equal to the recombination and $U=0$.

1. Depletion dark current

A CCD, however, is not operated in equilibrium. In the depletion region, beneath the CCD wells, the electric field sweeps holes to the p-type substrate and electrons to the potential wells. Thus there is a region depleted of carriers where n and $p \ll n_i$. Assuming the cross-sections for holes and electrons are equal ($\sigma_p = \sigma_n = \sigma$), Eq. (4) results in:

$$U_{dep} = \frac{\sigma v_{th} N_t n_i}{2 \cosh[(E_t - E_i)/kT]} \equiv \frac{n_i}{2\tau} \quad (6)$$

with:

$$\tau = \frac{\cosh[(E_t - E_i)/kT]}{\sigma v_{th} N_t} \quad (7)$$

as the effective generation-recombination life-time in the depletion region.

The generation-recombination rate, U , decreases exponentially as the energy level of the centers moves away from the mid-gap E_i . Hence, those centers close to E_i are most effective for producing dark current. Those centers close to the mid-gap are often referred to as deep-level impurities. For $E_t = E_i$, the carrier lifetime is given as:

$$\tau = (\sigma v_{th} N_t)^{-1} \quad (8)$$

Using Eq. (6), the dark current density per unit area generated in the depletion region can be expressed as:

$$I_{dep} = \frac{q x_{dep} n_i}{2\tau}, \quad (9)$$

where q is the electron charge and x_{dep} is the width of the depletion region. The dark current in electrons per pixel and per second, De_{dep}^- , is given as:

$$De_{dep}^- = \frac{x_{dep} A_{pix} n_i}{2\tau}, \quad (10)$$

where A_{pix} is the area of the pixel.

2. Diffusion dark current

The potential well beneath the gates does not reach all the way to the back-surface and a part of the CCD remains field-free. In this field-free region, the equilibrium minority carrier concentration n_{p0} is given as:

$$n_{p0} = \frac{n_i^2}{N_A}, \quad (11)$$

where N_A is the acceptor concentration in the p-type substrate, in our case boron.

We know from the study of diffusion current outside the space-charge region of a diode in reversed bias, that the diffusion current is proportional to the gradient of the electron concentration evaluated at the interface between the depletion and the neutral or field-free region:

$$I_{diff} = qD_n \left. \frac{dn_p}{dx} \right|_{x=0}, \quad (12)$$

where D_n is the diffusivity of electrons and n_p is the minority or electron concentration.

For a diode where the field-free region, x_{ff} , is generally larger than the diffusion length, L_n , the carrier concentration in the field free region is given as:

$$n_p = n_{p0} [1 - \exp(-x/L_n)] \quad (13)$$

which leads to

$$I_{diff, diode} = \frac{qD_n n_i^2}{N_A L_n} \quad (14)$$

However, it is questionable that the diffusion current as seen in a diode, describes the diffusion current in a back-illuminated CCD properly. Back-illuminated CCDs are thinned such that the field-free region is only a few microns. If the field-free region is smaller than the diffusion length, a carrier distribution which is not a function of the diffusion length but of the size of the field-free region might describe the system more accurately. Assuming

$$n_p = \frac{n_{p0} x}{x_{ff}} \quad (15)$$

leads to:

$$I_{diff} = \frac{qD_n n_i^2}{x_{ff} N_A} \quad \text{and} \quad De_{diff}^- = \frac{D_n A_{pix} n_i^2}{x_{ff} N_A}. \quad (16)$$

The expressions for the diffusion current in Eq. (14) and Eq. (16) are similar. The only change is that for a small field-free region, x_{ff} is substituted for L_n . The small field-free region might also have an impact on the diffusivity, D_n . Dark current, as described in Eq. (16), would result in an increasing diffusion current with decreasing field-free region. This cannot be true for very small values of x_{ff} . The minority carrier distribution given in Eq. (15) cannot describe such a system accurately. The boundary condition that the equilibrium carrier concentration is reached at the back surface cannot be true in such a case. For now, we will assume that the diffusion dark current for our CCD is similar to Eq. (14) and Eq. (16):

$$De_{diff}^- = \frac{D_n A_{pix} n_i^2}{x_c N_A} \quad (17)$$

where x_c is a characteristic length.

4. DATA ANALYSIS

The total dark current is given as the sum of the diffusion dark and the depletion dark current as given by Eq. (10) and Eq (17):

$$De^- = De_{diff}^- + De_{dep}^- = \frac{D_n A_{pix} n_i^2}{x_c N_A} + \frac{x_{dep} A_{pix} n_i}{2\tau} \quad (18)$$

The diffusion dark current is proportional to n_i^2 and the depletion dark current proportional to n_i . The temperature dependence of intrinsic carrier concentration is given by:

$$n_i = \sqrt{N_v N_c} \exp(-E_g/2kT) = 2 \left(\frac{2\pi k}{h^2} \right)^{3/2} m_e^{3/4} m_h^{3/4} T^{3/2} \exp(-E_g/2kT) = c_n T^{3/2} \exp(-E_g/2kT) \quad (19)$$

where h is Planck's constant, m_e and m_h are the effective masses of electrons and holes, and E_g is the band-gap for Si. Empirically, the band gap of Si is given as:¹⁶

$$E_g(T) = 1.17eV - \frac{4.73 \cdot 10^{-4} T^2}{T + 636} \quad (20)$$

The values of m_e and m_h for Si are not consistent throughout the literature. The values generally quoted for N_v and N_c at 300 K are: $N_v = 1.04 \cdot 10^{19} cm^{-3}$ and $N_c = 2.8 \cdot 10^{19} cm^{-3}$, which leads to: $c_n = 3.284 \cdot 10^{15} cm^{-3} K^{-3/2}$

It follows that the temperature dependence of the dark current can be expressed by the following equation:

$$De^- = \frac{D_n A_{pix} c_n^2}{x_c N_A} T^3 \exp(-E_g/kT) + \frac{x_{dep} A_{pix} c_n}{2\tau} T^{3/2} \exp(-E_g/2kT) \quad (21)$$

One can easily see that the first term increases in importance as the temperature increases. The second term will have a tendency to dominate at lower temperatures. It is commonly believed that the depletion dark current is dominant for temperatures close or smaller than room temperature.^{17,18} Hence, the activation energy for the dark current should be in the proximity of half the band-gap. The Arrhenius plot for the depletion current only would show a slight curvature due to the temperature dependence of the band-gap and the $T^{3/2}$ term. However, the curvature in our data is much stronger and the calculated activation energies are too high to be caused by the depletion dark current only. Figure 5 depicts the Arrhenius plot for the average dark current (average for all 222,784 pixels). The activation energy changes from about half the band gap at low temperatures to approximately the band gap at high temperatures. This indicates that a

transition from depletion to diffusion dominated dark current occurs in the investigated temperature range. The parameters for the diffusion dark current are specific to our particular camera but should not change significantly for different pixels on the chip. This explains why the dark current is fairly uniform for all pixels at high temperatures (see Fig. 2 and Fig. 4). In Fig. 4 the dark current is normalized such that the average dark current is set to 100 e⁻/sec. The distribution gets wider as the temperature increases. While the comparatively higher read noise at low temperatures, caused some spread in the distributions, the width increases mainly because of the increasing contribution of the depletion dark current. The dark current at low temperatures varies considerably due to the fact that the depletion current depends on the uneven impurity distribution.

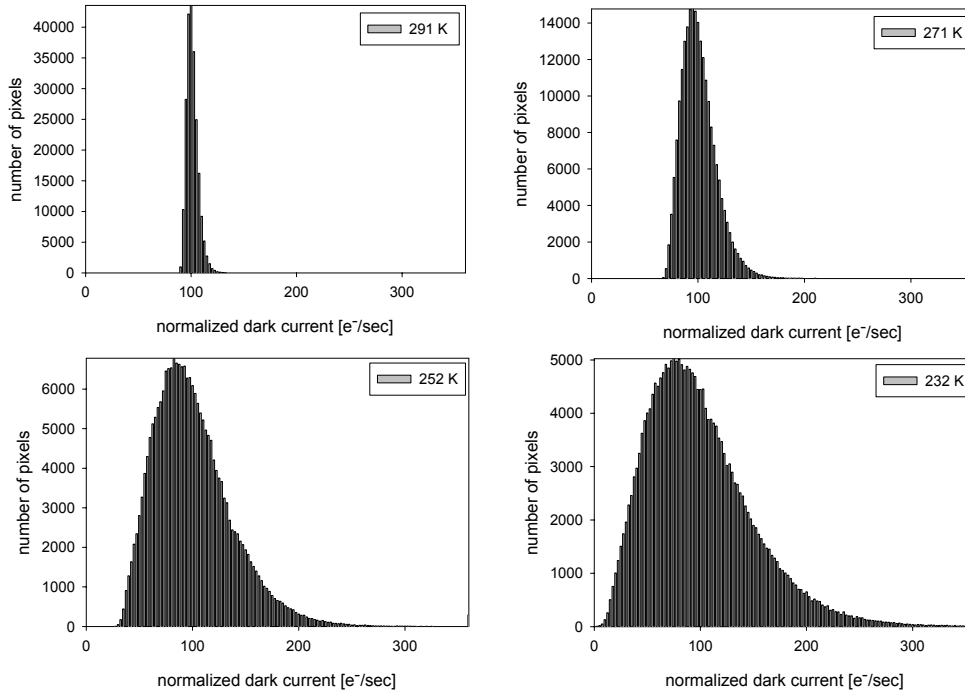


FIG. 4 Dark current histograms at 232 K, 252 K, 271 K and 291 K. The average dark current is normalized to 100 e⁻/s.

In order to verify if the dark current in our CCD can be described by Eq. (21), we left both prefactors and activation energies as parameters and fitted the data according to: $De^- = De_{0,diff}^- T^3 \exp(-\Delta E_{diff}/kT) + De_{0,dep}^- T^{3/2} \exp(-\Delta E_{dep}/kT)$

These trials showed that indeed the assumptions leading to Eq. (21) were justified and accordingly, we fixed the activation energies to E_g and $E_g/2$ respectively. Using only the two prefactors as fitting parameters showed that, as expected, $De_{0,diff}^-$ was very similar for all pixels. As seen in Fig. 6 the data could be accurately modeled with:

$$De^- = De_{0,diff}^- T^3 \exp(-E_g/kT) + De_{0,dep}^- T^{3/2} \exp(-E_g/2kT) \quad (22)$$

where E_g is the band gap of Si as given by Eq. (20), $De_{0,diff}^- = \exp(34.9) e^-/K^3$ and $De_{0,dep}^-$ is characteristic for each pixel. From Eq. (21) and Eq. (22) one gets

$$De_{0,diff}^- = \frac{c_n^2 A_{pix} D_n}{x_c N_A} \quad \text{and} \quad De_{0,dep}^- = \frac{x_{dep} A_{pix} c_n}{2\tau} \quad (23)$$

It is important to notice that the value for τ will be temperature dependent if the impurity centers are not located at mid-gap. Our analysis shows that impurities, roughly at mid-gap, are responsible for the depletion current. Modeling our data required only the assumption of different concentrations of mid-gap impurities. This does not exclude the possibility that different impurities located close to mid-gap are responsible for the electron generation. Such impurities could for example be Ni, Co, Au which are close to the mid-gap and to a lesser extent Fe which is further away from the mid-gap.¹⁹⁻²²

The characteristic length, x_c , derived from Eq. (23) is:

$$x_c = \frac{D_n c_n^2 A_{pix}}{De_{0,diff}^- N_A} \quad (24)$$

Our CCD was built of 30 Ωcm material. This leads to a acceptor impurity concentration N_A of approximately $4 \cdot 10^{14} \text{ cm}^{-3}$. The diffusivity, D_n , which in reality is temperature dependent, is more difficult to estimate than N_A . Assuming $D_n = 25 \text{ cm}^2/\text{s}$ results in a characteristic length x_c of 27 μm . This was larger than the field-free region which should be of the order of 10 μm or less, but much smaller than the diffusion length in Si. More research with various different sizes of the field-free regions is required to fully understand how the size of x_{ff} influences the diffusion current.

We can calculate the electron lifetime in the depletion region from Eq. (23) as:

$$\tau = \frac{x_{dep} A_{pix} c_n}{2De_{0,dep}^-} \quad (25)$$

The size of the depleted region for a buried-channel CCD can be estimated as described by Janesick.¹⁸ For an oxide thickness of 100 nm, an n-layer of width 1 μm and donor impurity concentration of $2 \cdot 10^{16} \text{ cm}^{-3}$, the 5 V bias leads to a depleted region, $x_{dep} = 8.6 \mu\text{m}$. The values for $De_{0,dep}^-$ varied for different pixels, its average value was given as $\exp(19) e^-/K^{3/2}$. This leads to an average lifetime of 0.05 s.

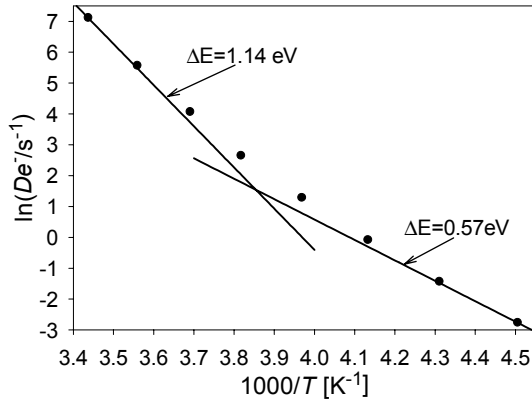


FIG. 5. The average of the logarithm of the dark current vs the inverse temperature.

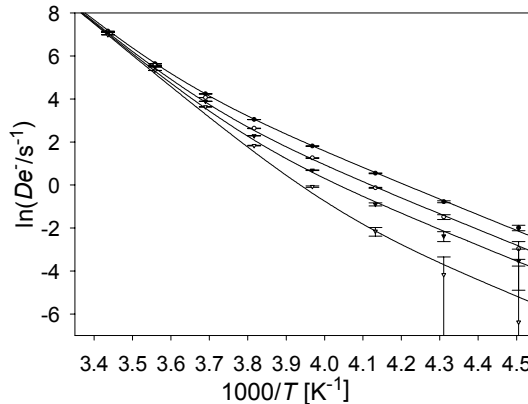


FIG. 6. The logarithm of the dark current vs the inverse temperature for four random pixels. The fits are based on the model assuming different impurity concentrations.

The deep-trap impurity concentration follows from Eq. (8) as: $N_t = (\sigma_{th} \tau)^{-1}$. The carrier velocity, though in reality temperature dependent, was assumed as 10^7 cm/s . The cross-section depends on the type of the impurity. As an

example, the cross-section of Au is equal to 10^{-15}cm^{-2} .^{21,22} This results in an average impurity concentration of approximately $2 \times 10^9/\text{cm}^3$ or about 10 impurities/pixel. Hot pixels have an impurity concentration twice or more of this average value.

5. CONCLUSION

In conclusion, we showed that analyzing dark current according to the Arrhenius law leads to a spread in the apparent activation energies with a mean value of approximately 1 eV. These activation energies and the corresponding prefactors were related as predicted by the MNR. The inversion in the dark current, for temperatures higher than the isokinetic temperature was not observed. We found that with increasing temperature the dark current for different pixels was getting more uniform. This could be explained by a transition from the depletion dark current to diffusion dark current with increasing temperature. The diffusion dark current was dominant at lower temperatures than commonly assumed. All dark current measurements could be modeled by different concentrations of a single impurity complex. It would be of general interest to understand how the diffusion dark current changes with different sizes of the field-free region.

6. REFERENCES

- ¹ R. Widenhorn, L. Mündermann, A. Rest, and E. Bodegom, *J. Appl. Phys.* **89**, 8179, 2001
- ² W. Meyer and H. Neldel, *Z. Tech. Phys.* **12**, 588, (1937)
- ³ D. G. Papageorgiou, G. A. Evangelakis, *Surface Science* **461**, L543, 2000
- ⁴ X. L. Wu, R. Shinar, and J. Shinar, *Phys. Rev. B* **44**, 6161, 1991
- ⁵ Y. Lubianiker and I. Balberg, *Phys. Rev. Lett.* **78**, 2433, 1997
- ⁶ K. Shimakawa and F. Abdel-Wahab, *Appl. Phys. Lett.* **70**, 652, 1996
- ⁷ Y. F. Chen and S. F. Huang, *Phys. Rev. B* **44**, 13775, 1991
- ⁸ H. Overhof and P. Thomas, "Electronic Transport in Hydrogenated Amorphous Semiconductors," (Springer-Verlag, Berlin, 1989)
- ⁹ A. Yelon, B. Movaghar and H.M. Branz, *Phys. Rev. B* **46**, 12244, 1992
- ¹⁰ A. Yelon and B. Movaghar, *Appl. Phys. Lett.* **71**, 3549, 1997
- ¹¹ R. Widenhorn, A. Rest, E. Bodegom, The Meyer-Neldel rule for a property determined by two transport mechanisms, to be published
- ¹² A. S. Grove, "Physics and Technology of Semiconductor Devices," (John Wiley & Sons, 1967)
- ¹³ C. T. Sah, R. N. Noyce, and W. Shockley, "Carrier Generation and Recombination in p-n Junction and p-n Junction Characteristics," *Proc. IRE*, **45**, 1228, 1957
- ¹⁴ R. N. Hall, "Electron-Hole Recombination in Germanium," *Phys. Rev.* **87**, 387, 1952
- ¹⁵ W. Shockley and W. T. Read, "Statistics of the Recombination of Holes and Electrons," *Phys. Rev.* **87**, 835, 1952
- ¹⁶ S.M. Sze, "Physics of Semiconductor Devices," second edition (John Wiley & Sons, 1981)
- ¹⁷ M. J. Howes and D. V. Morgan, "Charge-Coupled Devices and Systems," (John Wiley & Sons, 1979) p. 17
- ¹⁸ J. R. Janesick, "Scientific Charge-Coupled Devices," Spie Press, 2001
- ¹⁹ R. D. McGraph, J. Doty, G. Lupino, G. Ricker, and J. Vallerga, *IEEE Trans. Electron Devices*, vol. ED-**34**, 2555, 1987
- ²⁰ W. C. McColgin, J. P. Lavine, J. Kyan, D. N. Nichols, and C. V. Stancampiano, International Electron Device Meeting 1992, p. 113, 13-16 Dec., 1992
- ²¹ W. C. McColgin, J. P. Lavine, and C. V. Stancampiano, *Mat. Res. Soc. Symp. Proc.* **378**, 713, 1995
- ²² W. C. McColgin, J. P. Lavine, C. V. Stancampiano, and J. B. Russell, *Mat. Res. Soc. Symp. Proc.* **510**, 475, 1998